J Appl Electrochem (2013) 43:73–83
DOI 10.1007/s10800-012-0501-6

ORIGINAL PAPER

Infilling of porous materials with various polymorphs of calcium carbonate by an electromigration technique

R. D. Moser · O. L. Rodriguez · R. G. Hidalgo-Hernandez · P. G. Malone · M. Q. Chandler · P. G. Allison · C. A. Weiss Jr. · Kevin Torres-Cancel

Received: 8 August 2012 / Accepted: 29 October 2012 / Published online: 8 November 2012

Abstract Recent interest in bio-inspired materials has led to the development of techniques that can be used to synthesize hierarchical structures with controlled morphology and mineralogy. One such technique investigated in this study consists of the use of electromigration and electrodeposition techniques to deposit mineral phases with controlled morphology and mineralogy by infilling a predefined porous templates. Here, the utility of precipitating various polymorphs of calcium carbonate in three-dimensional templates is demonstrated. Applied potentials and times were varied while scanning electron microscopy and X-ray diffraction were used to determine polymorph formed and its morphology. It was found that higher applied potentials and shorter operating times resulted in the formation of metastable polymorphs of calcium carbonate (e.g., vaterite) that infilled the porous media. Results provide insights for developing bio-inspired composite materials for various structural and medical applications, such as synthetic bone.

Keywords Electromigration · Calcium carbonate · Biomimetic · Biomedical applications

R. D. Moser (✉) · R. G. Hidalgo-Hernandez · P. G. Malone · M. Q. Chandler · P. G. Allison · C. A. Weiss Jr. · K. Torres-Cancel
Geotechnical and Structures Laboratory, U.S. Army Engineer Research and Development Center, Halls Ferry Rd, Vicksburg, MS 39180, USA
e-mail: robert.d.moser@usace.army.mil

O. L. Rodriguez
Department of Mechanical Engineering, University of Puerto Rico, Mayagüez, PR 00680, USA

1 Introduction

Methods to synthesize biomimetic and bio-inspired materials which exhibit hierarchical nano- and micro-scale structures with controlled morphology and mineralogy offer opportunities to develop novel materials [1]. Electromigration and electrodeposition techniques are gaining increasing consideration as a material processing method to synthesize these hierarchical structures [2]. This increased interest results from the ease of use and ability to synthesize composite systems of a variety of materials [3]. In techniques such as electrophoresis and electromigration, an imposed electric field acts as the driving force for the movement of ions or particles suspended in a solution, driving them through non-conductive porous media toward the electrode of opposite charge to form solid deposits.

A variety of techniques have been used successfully and have demonstrated the practicality of electromigration techniques in producing coatings, laminated or graded materials, and in the infiltration in porous templates [4]. When used as a coating deposition technique, materials can be added to a surface to produce specific enhanced properties [5–7]. For example, the application of electrophoresis can be used to produce surfaces with selected properties such as improved wear and oxidation resistance, bioactive coatings for medical implants, and functional coatings for electronic, magnetic, and related applications [8].

Morefield et al. [9], Ma et al. [10], and Chen et al. [11] described the use of an electromigration system to infiltrate ions or particles into a porous template for structural, tissue engineering, and microfiltering applications. The success of the electromigration procedures in coating deposition of layered composites and infiltration of porous media has demonstrated that this approach can be a suitable synthesis technique for microscale and nano-scaled structurally unique

composites. Of particular interest in this paper is the development of bio-inspired composites that can be synthesized by electromigration techniques in predefined three-dimensional templates that mimic those found in the microscale brick-and-mortar structure of nacre [12] and functional gradations present in mineralized fish scales [13, 14]. Similar studies have demonstrated the ability of electromigration techniques for controlled deposition of calcium carbonate precipitates of the polymorphs vaterite and calcite [15]. Here we extend these techniques to precipitation in the predesigned three-dimensional porous templates.

The work reported here presents techniques for electromigration and precipitation of calcium carbonate in structured templates including microporous polycarbonate membranes and polyethylene foams. Parameters related to the electromigration process and their effects on the mineral phase and morphology were investigated, including applied cell potential and test duration. The morphology and mineralogy of the precipitated calcium carbonate was characterized using Scanning Electron Microscopy (SEM) and X-Ray Diffraction (XRD). These preliminary studies are directed toward producing mineral/polymeric composites for structural and biomedical applications. Infilling solvent-removable polymeric materials (such as polycarbonate) allows the electromigration technique to become a technique for investment casting a variety of intricate mineral porous media for biological and industrial applications.

2 Experimental

Ammonium carbonate $(NH_4)_2CO_3$ and calcium acetate $Ca(C_2H_3O_2)_2$ were used as the reactants for the calcium carbonate ($CaCO_3$) precipitation that was produced by electromigration between two solutions separated by a porous template (polycarbonate membrane or polyethylene foam). Microporous polycarbonate membranes and medium-density polyethylene (MDPE) foam specimens were used as the porous organic templates. Commercial rigid plastic filter holders were modified to produce two non-conducting reagent reservoirs separated by a disk made from the porous organic medium sealed across the interface between the reactants. Carbon electrodes were used to make electrical contact with the solutions in the reagent reservoirs and a low-voltage electrical power supply was used to produce a potential across the membrane. The kinetics of the electromigration-precipitation process could be changed by varying the potential difference across the membrane and the time the potential was applied across the membrane. The morphology and structure of the electrodeposited crystallites was investigated by SEM and XRD techniques.

2.1 Materials

Solutions were prepared from analytical grade $(NH_4)_2CO_3$ and $Ca(C_2H_3O_2)_2$ at concentrations of 0.5 M in deionized H_2O. Each 0.5 M solution of reactants was prepared at room temperature (25 °C) with constant stirring until all reagents were fully dissolved.

Nuclepore polycarbonate membranes (47 mm diameter, $\approx$22 μm thickness) and MDPE foam (39 mm diameter, 5 mm thickness) specimens were used as the porous templates. Both template materials are non-conductive substrates. SEM micrographs were used in conjunction with image analysis software (ImageJ) to determine the average

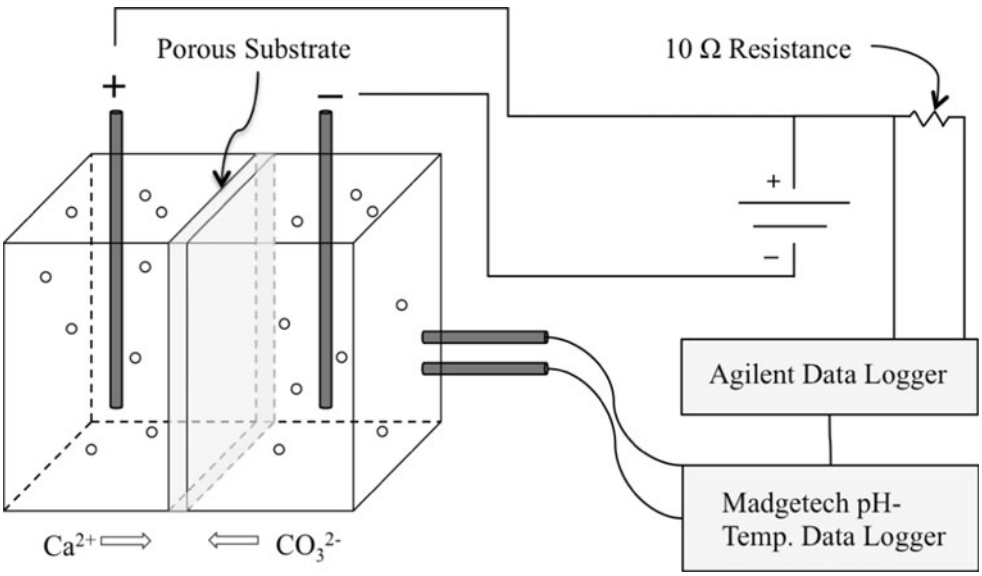

Fig. 1 Electromigration cell experimental setup schematic

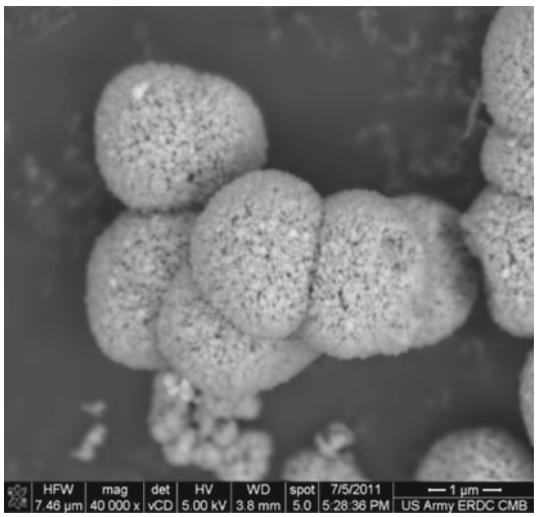

(a) Botryoidal agglomerations of vaterite nanoparticles

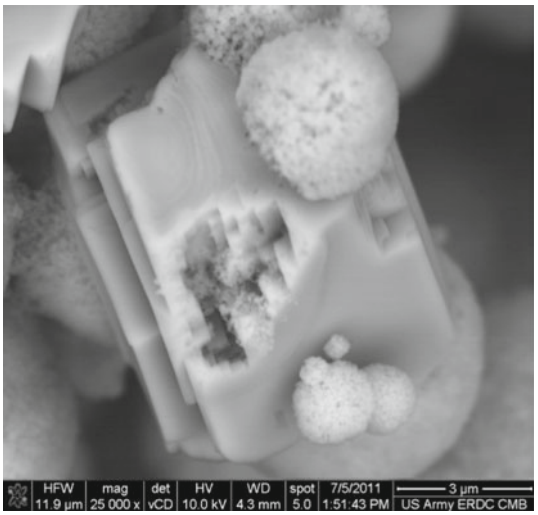

(b) Transformation of vaterite nanoparticles into calcite rhombs

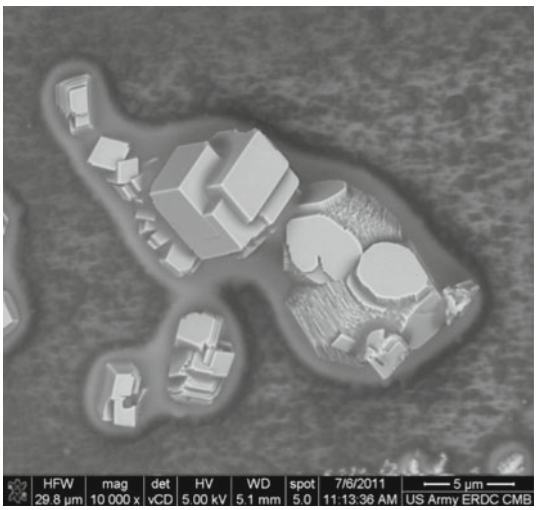

(c) Transformation of amorphous calcium carbonate to calcite rhombs

Fig. 2 Polymorphism observed in electrodeposited precipitates of $CaCO_3$

pore diameter and density (pores/area) of the polycarbonate films. The calculated average pore diameter for the polycarbonate membranes was 8.81 ± 1.43 μm, which is in accordance with the value reported by the manufacturer (8 μm pore diameter). The average pore density was 900 pores mm^2, and the pore area to film area ratio was 5.47 %. The MDPE foam specimen was measured using the ASTM C642-06 [16] standard as a reference standard to determine the void space volume fraction.

2.2 Electromigration experimental setup

A commercial Nalgene® MF-75 series filter holder unit acted as the electromigration cell. Each unit included two fluid reservoirs (500 ml each) in which the $CaCO_3$ forming reagents were deposited; the porous template served as the interface between them. The polycarbonate membranes were accommodated on the holder's analytical support plate, and the MDPE foam samples were clamped in a support plate replacement collar. The chamber cover, supporting plate, replacement collar O-rings, and MDPE foam specimen circumference were silicone grease sealed. Acrylic bases were custom made to maintain the Nalgene® filter holder in a horizontal position.

Graphite rod electrodes were used to apply voltage across the cell. The anode was located in the $Ca(C_2H_3O_2)_2$ solution chamber, and the cathode was positioned in the $(NH_4)_2CO_3$ chamber. Both electrodes were placed at 70.0 mm from the porous template. A schematic of the experimental setup is presented in Fig. 1. The large distance of the electrode relative to the lateral dimensions of the porous template was used to improve the uniformity of the applied electric field present.

A regulated power supply delivered a constant voltage to each Nalgene® station. For the polycarbonate membranes, a cell potential of 5.0, 10.0, and 20.0 V was applied with testing durations of 2, 3, and 6 h. Experimental conditions of 10.0, 20.0, and 30.0 V with duration periods of 2, 6, or 12 h were applied to the MDPE foam samples. At the end of the deposition time, the specimens were extracted from the electromigration cell with tweezers and let dry at 25 °C for 48 h.

An Agilent data acquisition unit recorded the voltage drop across a 10 Ω resistor to allow the flow of current to be monitored. Agilent BenchLink Data Logger software was employed to generate voltage drop vs. time plots. Madgetech® data logger collected solution temperature and pH data. Both the pH and the temperature probes were positioned on the $Ca(C_2H_3O_2)_2$ solution chamber.

2.3 Characterization techniques

An FEI Nova NanoSEM 630 field emission environmental SEM was used to investigate the morphology of the

specimens. The specimens were analyzed using a back-scattered electron detector (vCD). Accelerating voltages ranged from 5 to 15 kV. Samples were imaged in low-vacuum (0.1–1.0 mbar) to minimize charging effects.

XRD patterns for the washed and sieved specimens were obtained using a PANalytical Ẋpert powder diffractmeter (Co anode) operating at a voltage of 45 kV and current of 40 mA. Care was taken to avoid grinding the samples, a procedure that can alter the mineralogy. Data were collected at a 2°2θ angle ranging from 2 to 70°2θ. The specimens were positioned above zero background plates and covered with kapton films. Ẋpert High Score Plus and MDI Jade 2010 analysis software with access to ICDD reference databases were used for qualitative phase identification.

3 Results and discussion

3.1 Morphology of electrodeposited $CaCO_3$

Calcium carbonate, the mineral phase investigated in the present study, is known to form in three crystalline polymorphs—vaterite (hexagonal), aragonite (orthorhombic), and calcite (trigonal)—and an amorphous form. In the present study, electrodeposited precipitates of $CaCO_3$ resulting from electromigration between calcium acetate and ammonium carbonate solutions were primarily botryoidal agglomerates of vaterite nanoparticles (Fig. 2a), larger rhombohedral formations of calcite (Fig. 2b), or amorphous calcium carbonate (Fig. 2c). Photomicrographs indicate the more stable polymorphs (i.e., calcite) formed via Ostwald ripening from less stable forms like vaterite and amorphous calcium carbonate (Figs. 2b, c) as is classically thought to occur [17]. The presence of metastable polymorphs of $CaCO_3$ present in electrodeposited precipitates suggests that the electromigration technique used has an effect on the kinetics of the crystallization process that in turn can produce changes in crystal morphology and mineralogy. The following sections illustrate the effect of cell potential, charging time, and the confinement caused by the porous template on the crystal morphology and mineralogy of carbonates formed in polycarbonate membranes and polyethylene foams.

3.2 Electromigration and precipitation of $CaCO_3$ in polycarbonate membranes

The relationship between cell current (on a logarithmic scale) and duration of applied cell potentials of 5, 10, and 20 V is shown in Fig. 3. Initial currents roughly corresponded to the magnitude of the applied cell potential, with higher cell potentials (e.g., 20 V) yielding higher currents. However, the measured current quickly deviated from this trend as the deposition of $CaCO_3$ occurred and began to infill the pore spaces in the polycarbonate membrane. Ionic mobilities of Ca^{2+} and CO_3^{2-} of interest in the present study are in the range of 5×10^{-4}–8×10^{-4} m/s

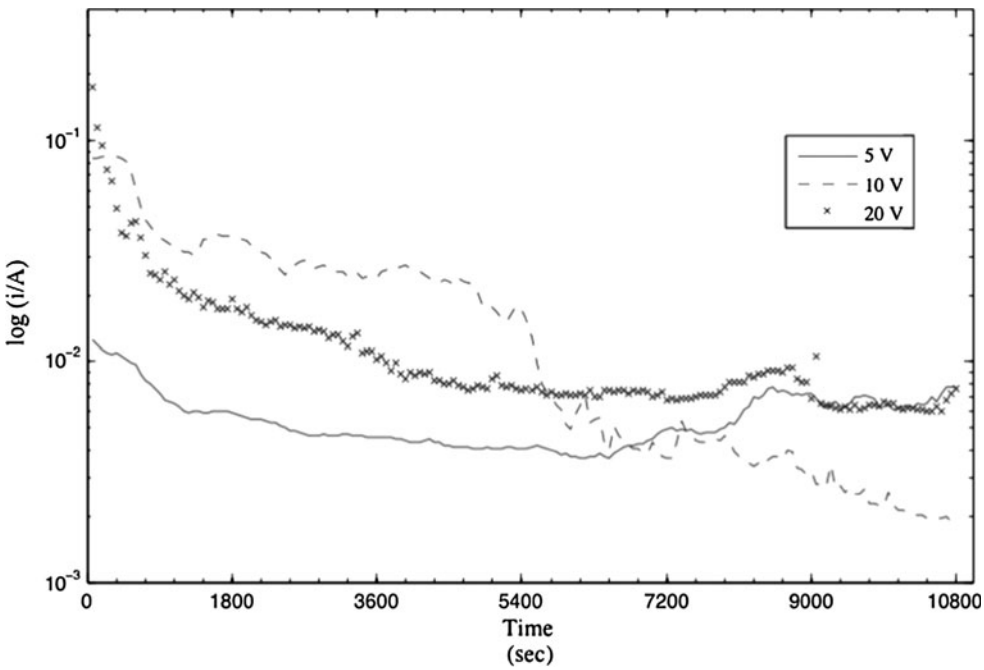

Fig. 3 Current versus time relationship for the calcium carbonate deposition process in polycarbonate substrates

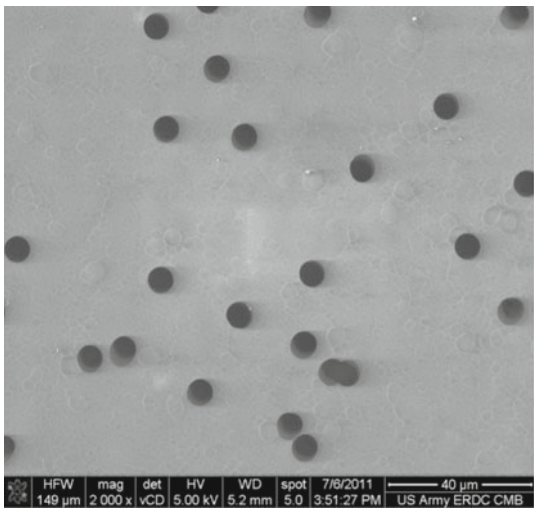

(a) Polycarbonate membrane prior to testing

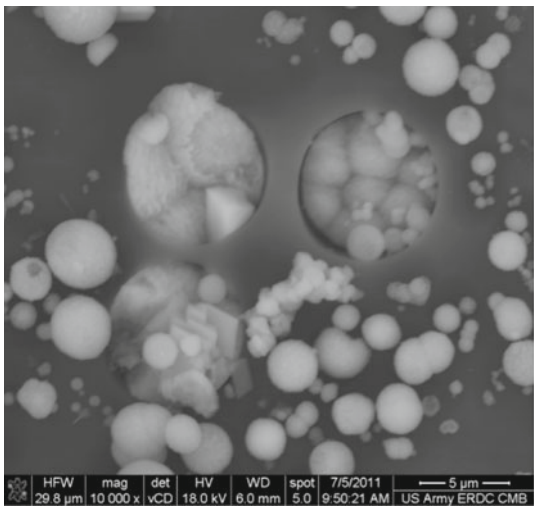

(b) Infilling of pores with metastable vaterite

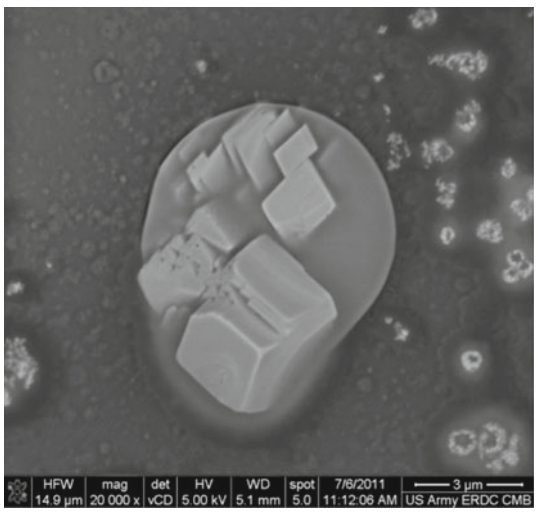

(c) Ostwald ripening of metastable phases in pore to form calcite

Fig. 4 Infilling of pores in polycarbonate membrane

Table 1 Calcium carbonate—polycarbonate specimens weight distribution by applied potential difference. Deposition time: 3 h

Cell potential difference (V)	Mass (g)[a]	Δ Mass %[b]
5	0.0348 ± 0.0071	+159.47
10	0.0438 ± 0.0043	+226.58
20	0.0415 ± 0.0113	+209.43

[a] Post-deposition process mass. The values presented are the average of five specimens with standard deviation

[b] Compare to the polycarbonate template average mass, 0.0130 ± f0.0015 g

[18] for applied electric fields of 100 V/cm. With a known cell geometry with 14 cm separation between electrodes, the electric field strength in the present study is 0.36, 0.71, and 1.43 V/cm for applied cell potentials of 5, 10, and 20 V, respectively. As a result, the anticipated migration rates are approximately 1.5, 3, and 6 µm/s for applied cell potentials of 5, 10, and 20 V, respectively. Based on these estimates, it requires approximately 13, 6.5, and 3.25 h for full ion exchange between each side of the electromigration cell for applied cell potentials of 5, 10, and 20 V. These estimates support the finding that reductions in current occurred more rapidly in experiments operated at higher cell potentials, causing a more rapid migration of Ca^{2+} and CO_3^{2-} toward the porous membrane and subsequent infilling with solid $CaCO_3$ that led to an increase in resistance and decrease in current between the anode and cathode. SEM micrographs shown in Fig. 4 indicate that as the originally open pores (Fig. 4a) become filled with various polymorphs of $CaCO_3$ (Figs. 4b, c), the ionic connectivity between the anodic and cathodic portions of the electromigration cell are effectively locally cutting off in that area. Along with the rapid decrease in current with time, erratic shifts in current were observed as the pores transform from open ionically conductive pathways to filled resistive pathways due to the ion transport and the deposition of $CaCO_3$. Erratic shifts in current were minimal at the 5 V applied cell potential which is likely due to its lower rate of ion migration and subsequent slower infilling with precipitated $CaCO_3$ in the pore spaces of the polycarbonate membrane. Currents remaining at the end of the testing duration indicate that, while pore infilling significantly reduced the ionic conductivity of the system, it is likely that small proportions of pores remain open and available for ion transport.

Additional sensors monitored during the test confirmed a constant temperature of 24 °C and pH of 8.8–9.0 measured in the cathodic portion of the electromigration cell. It is possible that acidification occurred in the anodic portion of the electromigration cell due to electrolysis

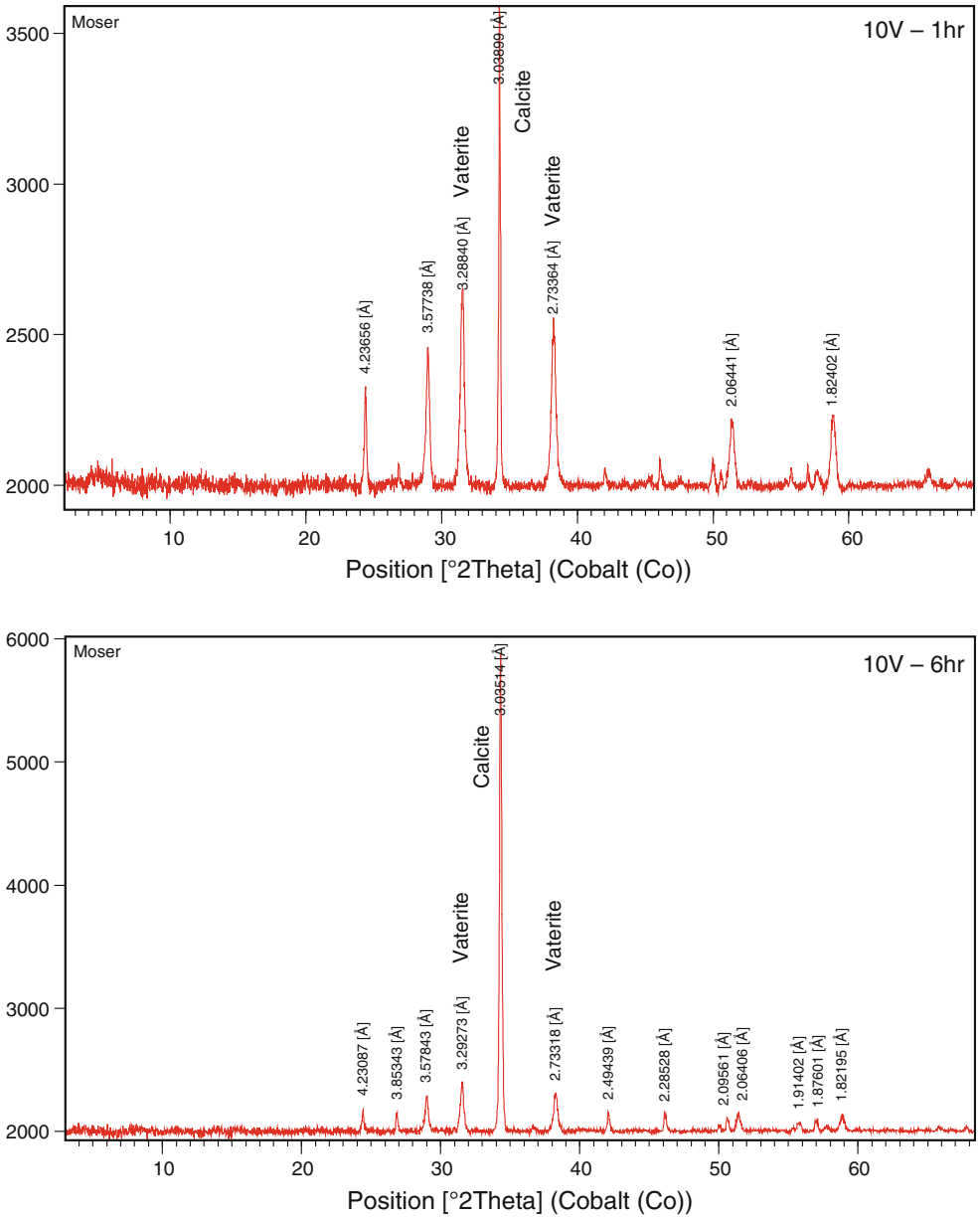

Fig. 5 Comparison of $CaCO_3$ formed under 10 V applied cell potential with testing duration of 1 and 6 h

processes. However, these measurements of pH were made at the cathode. Temperature and pH are known to have a significant influence on which polymorph of $CaCO_3$ is formed and its stability. Previous studies have shown that the formation of calcite and vaterite is promoted at pH values less than 10 and greater than 12, while the formation of aragonite is promoted at pH of approximately 11 [19, 20]. Supersaturated solutions have been shown to produce amorphous $CaCO_3$ [21]. In the case of the present study, vaterite and calcite, which are anticipated at pH values below 10 were observed along with amorphous $CaCO_3$. This suggests that the presence of an electric field as the driving force for ion movement has an influence of morphology and mineralogy of precipitated $CaCO_3$ and also promotes the formation of amorphous $CaCO_3$ that typically only form under supersaturated conditions.

In order to quantitatively compare specimens with different cell potential differences, a $CaCO_3$ saturation criterion was established; that is the current drop at which it was found that all of the pores were infilled with $CaCO_3$. When the decaying current curve reached 10 % of its first

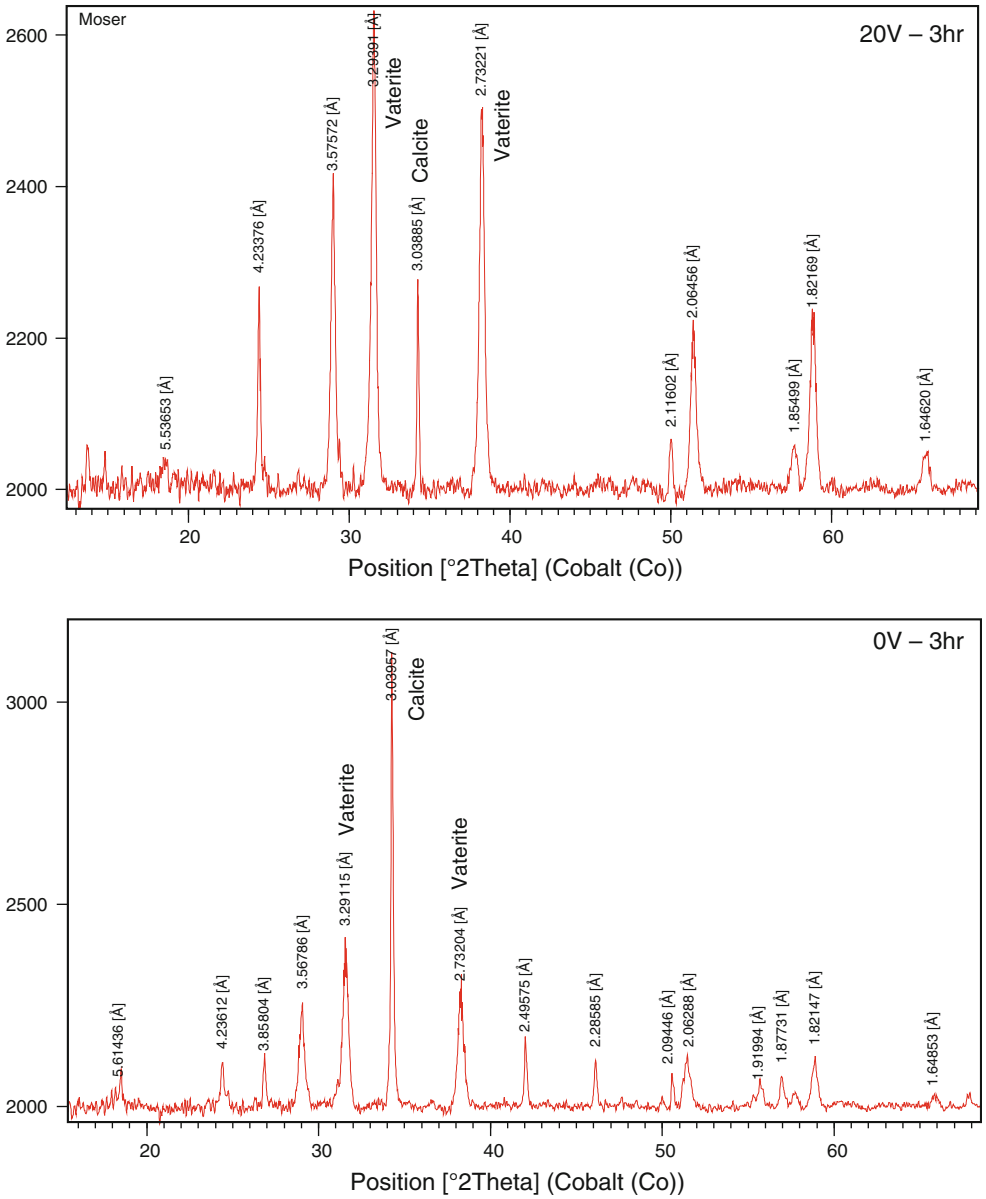

Fig. 6 Comparison of $CaCO_3$ formed under 20 and 0 V applied cell potential over a 3 h test duration

measured value, the template was considered filled. In addition, the amount of $CaCO_3$ precipitated on the polycarbonate membrane was quantitatively determined by mass measurements of pre- and post-deposition specimens. Results of these measurements are presented in Table 1. An increase in mass associated with the formation of $CaCO_3$ on the membrane surface and infilling of the pores was observed. However, there were no clear trends between amount of $CaCO_3$ deposited and applied cell potential. The lack of relationship between deposited mass of $CaCO_3$ and applied cell potential likely results from loss of precipitated $CaCO_3$ from the porous template during its removal from the electromigration cell. This becomes particularly important when a majority of the deposition occurs on the surface of the porous template rather than in the pore space due to unequal rates of ion migration.

Finally, the influence of applied cell potential and time on $CaCO_3$ polymorphism was examined. Results of SEM imaging and XRD analyses confirmed that these voltage and duration do influence which polymorph of $CaCO_3$ forms, with metastable vaterite precipitation occurs preferentially under higher applied cell potentials and lower

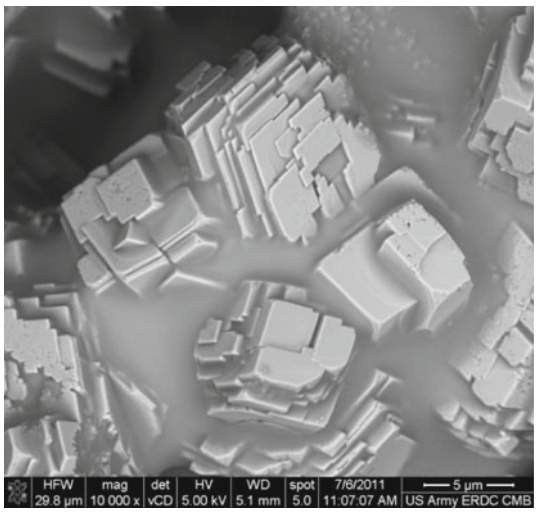

(a) Stable calcite rhombs formed from amorphous calcium carbonate at an applied cell potential of 5 V and test duration of 2 hrs

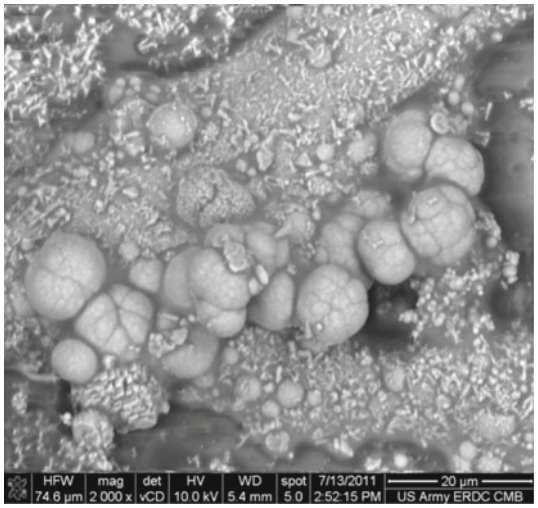

(b) Amorphous $CaCO_3$ and botryoidal agglomerates of vaterite nanoparticles formed at an applied cell potential of 20 V and test duration of 2 hrs

Fig. 7 Influence of applied cell potential on $CaCO_3$ polymorphism

Table 2 Calcium carbonate—medium-density polyethylene foam samples weight distribution by applied potential difference. Deposition time: 6 h

Cell potential difference (V)	Mass (g)[a]	Δ Mass %[b]
10	0.8883 ± 0.0046	+37.30
20	0.8237 ± 0.1287	+27.32
30	0.9108 ± 0.0811	+40.77

[a] Post-deposition process mass. The values presented are the average of five specimens with standard deviation

[b] Compare to the medium-density polyethylene foam template average mass, 0.6470 ± 0.0670 g

test durations. The XRD patterns presented in Fig. 5 demonstrate the increased presence of vaterite at shorter test durations in specimens synthesized with a 10 V applied cell potential. The XRD patterns in Fig. 6 demonstrate the influence of applied cell potential, with the increase in vaterite formation at 20 vs. 0 V over a 3 h test duration. SEM imaging confirmed the trends in crystal polymorph formed (see Fig. 7). Previous direct-from-solution precipitation experiments, where no electromigration system was employed, have found that the presence of a porous template like that investigated here inhibited the formation of amorphous calcium carbonate and promoted the formation of vaterite and its subsequent transformation into calcite via Ostwald ripening [22]. In the present study where an applied electric field was present, both amorphous calcium carbonate and vaterite were observed in confined pore spaces in the template and both were partially transformed into calcite rhombohedra. This observation suggests that the electromigration and deposition procedure used in this investigation also aids in the formation of specific polymorphs of $CaCO_3$, including amorphous $CaCO_3$, and can preferentially deposit these mineral phases into a three-dimensional porous template of known geometry. The unstable current density at the higher voltage as shown in Fig. 3 may have also contributed to the formation of metastable polymorphs such as vaterite as shown in Fig. 7, since the unstable current density affects the quality of the deposits as suggested by Yanagishita and coworkers [23].

3.3 Electromigration and precipitation of $CaCO_3$ in polyethylene foams

In addition to tests performed in a thin polycarbonate membrane, the novel electromigration and precipitation technique was also investigated for infilling of three-dimensional porous templates, such as an MDPE foam. Figure 8 shows representative results of the current versus deposition time relationship for the MDPE foam specimens. The cell geometry used to evaluate the infilling of the MDPE foams was the same as that used for the polycarbonate membranes; thus, ion migration rates are anticipated to be similar in this system. Similar behavior as in the polycarbonate membranes was observed in the MDPE foam specimens, with a decrease in current with time as the pore space begins to infill with $CaCO_3$. The decrease in current was more gradual compared with the polycarbonate membranes. This effect is likely due to the larger pore sizes and greater pore interconnectivity that lessens the tendency for the infilling of pores to block ion migration through the membrane.

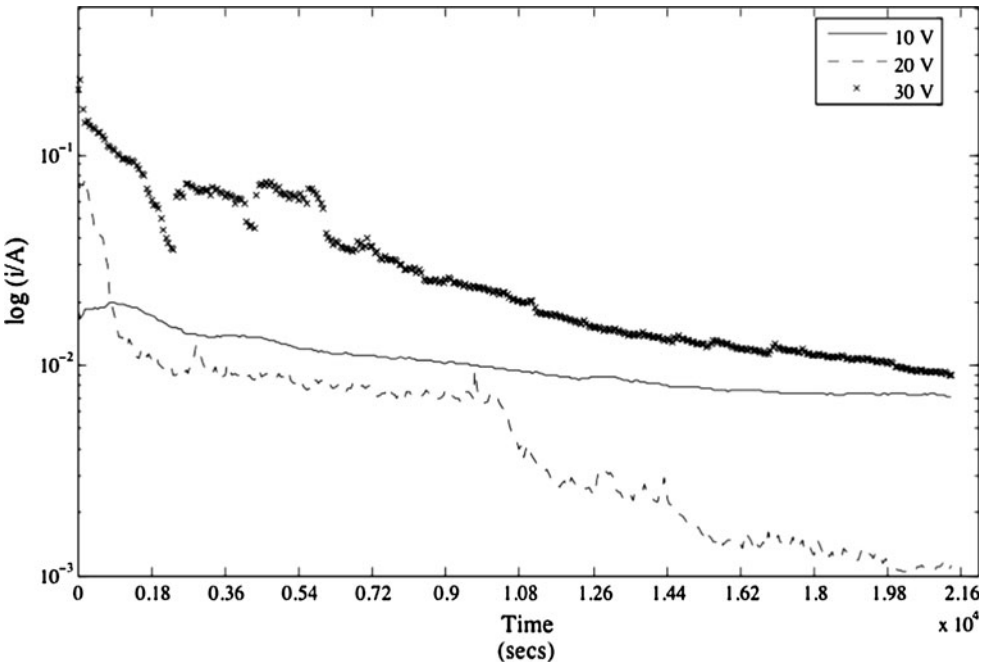

Fig. 8 Current–time relationship for the calcium carbonate deposition process in medium-density polyethylene foam substrates

Measurements of mass gain presented in Table 2 demonstrate the increase in mass observed in MDPE foams following testing. However, like the polycarbonate membranes, no clear relationship between applied cell potential and mass gain can be demonstrated. Similar to the polycarbonate membranes, the factors that are influencing the mass measurements and their correlation with applied cell potential likely are the poor cohesion between $CaCO_3$ and the MDPE substrate and the handling of the specimens after the deposition and removal from the electromigration cell.

SEM imaging of the MDPE foams following the testing duration revealed a partial infilling of the pore spaces with $CaCO_3$ (Fig. 9). However, infilling was observed to occur preferentially on the cathodic side of the electromigration cell as can be observed in the specimen cross section shown in Fig. 10. Imaging of five randomly selected sites along a sliced cross section of the foam showed the thickness of this deposited layer to be approximately 300–500 μm, which is approximately 10 % of the total specimen thickness. This result suggests that, in this system and under the applied cell potentials studied, the ionic mobility of Ca^{2+} ions is higher when compared with CO_3^{2-} and shifts the reaction front to the $(NH)_4CO_3$ solution side of the electromigration cell. Results from studies of the MDPE foams demonstrated the difficulty of fully infilling a 3D matrix. As a result, the current cell design may be limited to thin coatings or 3D structures where infilling of pores does not severely limit subsequent electrodeposition events. In addition, adequate knowledge of ion mobilities and proper cell geometries are necessary to ensure that the reaction front present in the electromigration cell is properly positioned within the porous template.

3.4 Utility for producing predefined 3D structures

Results of the studies presented herein conducted on polycarbonate membranes and MDPE foams demonstrated the ability to infill a template material with a mineral phase by an electromigration technique between two reactive solutions. One potential useful application for such a technique is the ability to remove the template in a "lost wax" type of system, leaving behind a mineral-based structure with controlled geometry that is the negative of the template. Here, the removal of the template material following deposition (e.g., using an appropriate solvent to dissolve the template) was used to reveal internal three-dimensional structures present in the polycarbonate membrane by dissolving it in a solvent. Here methylene chloride (CH_2Cl_2) was used to dissolve the polycarbonate. Typical structures resulting from removal of the polycarbonate membrane consisted of $CaCO_3$ micropillars attached to a $CaCO_3$ thin film as shown in Fig. 11. Potential future applications for this technique include synthesis of three-dimensional structures of mineral phases such as $CaCO_3$ (e.g., biomimetic materials), hydroxyapatite (e.g., artificial bone), or other synthetic materials in predefined, removable, porous templates.

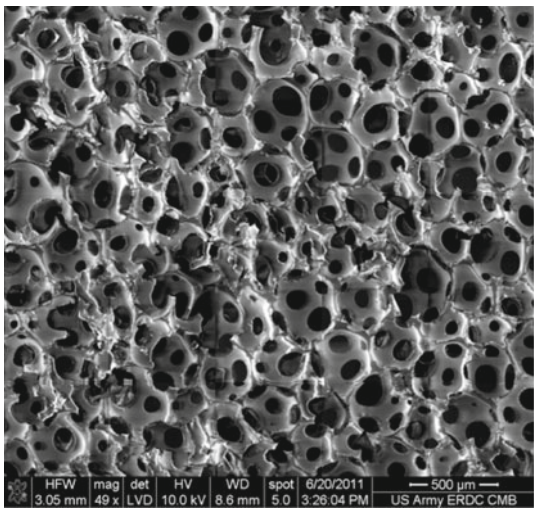

(a) MDPE foam prior to testing with voided porosity

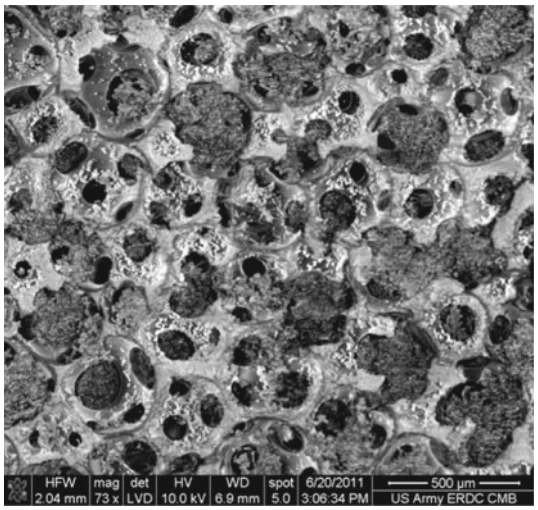

(b) Surface of MDPE foam following testing at an applied cell potential of 15 V and 12 hrs test duration with precipitated $CaCO_3$ in pore space

Fig. 9 MDPE foam specimen before and after electromigration experiment

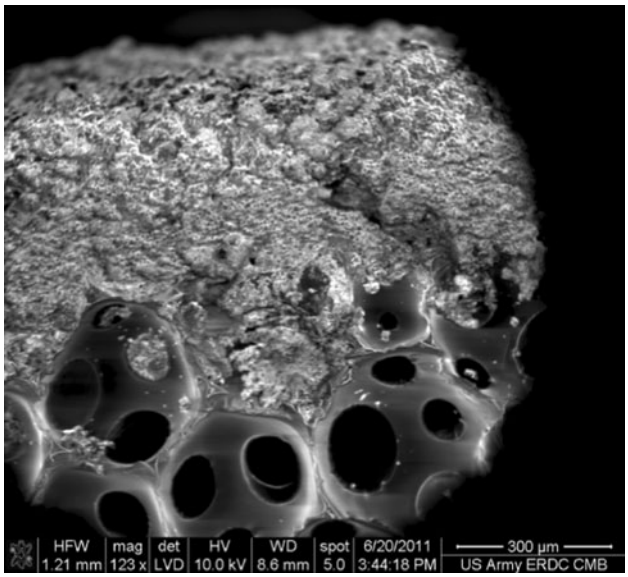

Fig. 10 *Cross section* of MDPE foam specimen showing preferential deposition on carbonate side of electromigration cell containing the cathodic electrode

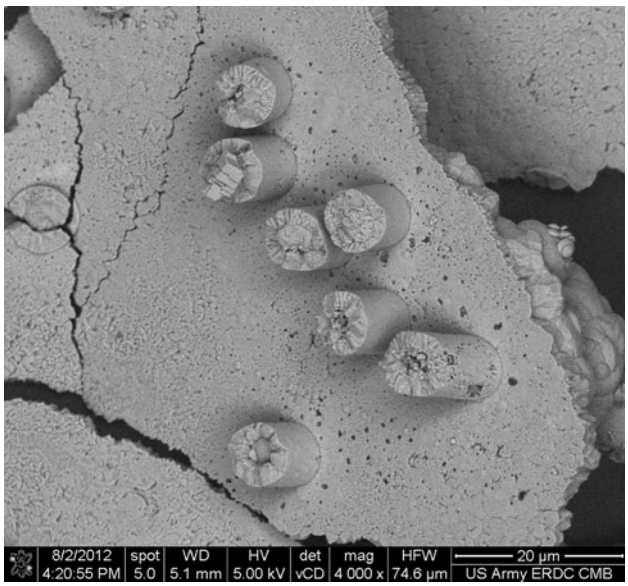

Fig. 11 Micropillars of $CaCO_3$ formed by infilling of polycarbonate membrane and liftoff of membrane to reveal templated mineral deposit

4 Conclusions

In this research, the use of electromigation was demonstrated as a method to deposit $CaCO_3$ in porous materials, including polycarbonate membranes and MDPE foam. Electrodeposited $CaCO_3$ was characterized using SEM and XRD analyses. The primary conclusions of the study are:

- The use of electromigration to promote the movements of oppositely charged reactive ions toward a reaction front is an effective method to infill porous materials with a mineral phase.
- Higher applied cell potentials and shorter test durations resulted in an increase in the proportion of metastable phases such as vaterite and amorphous calcium carbonate. Lower potentials and longer durations promoted the transformation of metastable phases to stable calcite via Ostwald ripening.
- The electrodeposition process is self limited by reductions in the ionic conductivity between the anodic and cathodic portions of the electromigration cells as the individual pores are infilled with the mineral phase.

- Three-dimensional porous materials with increased thickness (i.e., the MDPE foam investigated) present a challenge that the location of the anode and cathode and geometry of the electric field between each electrode must be calculated accurately based on ionic mobility (in this case for Ca^{2+} and CO_3^{2-}) to ensure that the reaction front is within the porous template.
- Extending this electromigration and deposition technique to other porous templates and materials may have many applications in the fields of biomimetic materials, artificial implants, and bone regeneration where techniques for synthesizing micro- and nano-scale structured mineral phases are needed.
- Future work should focus on extending this technique to other porous templates (e.g., nacre-inspired three-dimensional brick-and-mortar structures) and investigating other infilling materials such as hydroxyapatite. Numerical modeling of ion transport in porous templates under an electric field also need to be performed to provide understanding on the relationship between the solid infilling and different parameters such as applied voltage, the distance between the surfaces of the templates to the electrodes, and pore connectivity.

Acknowledgments The Authors would like to acknowledge the support for this work provided by the U.S. Army ERDC Center-Directed Research Program. The Authors would also like to thank the staff and facilities of the Geotechnical and Structures Laboratory's Concrete and Materials Branch for supporting the experimental work. Permission to publish was granted by Director, Geotechnical and Structures Laboratory, U.S. Army Engineer Research and Development Center.

References

1. Qiao L, Feng Q, Lu S (2008) In vitro growth of nacre-like tablet forming: from amorphous calcium carbonate, nanostacks to hexagonal tablets. American Chem Soc 8(5):1509–1514
2. Van der Biest O, Vandeperre L, Put S, Anne G, Vleugels J (2006) Laminated and functionally graded ceramics by electrophoretic deposition. Adv Sci Tech 45:1075–1084
3. Boccaccini AR, Keim S, Ma R, Li Y, Zhitomirsky I (2010) Electrophoretic deposition of bio-materials. J Roy Soc 7(5):581–613
4. Bersa L, Liu M (2007) A review on fundamentals and applicattions of electrophoretic deposition (EPD). Prog Mater Sci 52(1):1–61
5. Boccaccini AR, Zhitomirsky I (2002) Application of electrophoretic and electrolytic deposition techniques in ceramics processing. Curr Opin Solid State Mater Sci 6(3):251–260
6. Sarkar P, Nicholson P (1996) Electrophoretic deposition (EPD): mechanisms, kinetics and application to cereamics. J Am Ceram Soc 79(8):1987–2002
7. Van der Biest O, Vandeperre LJ (1999) Electrophoretic deposition of materials. Annu Rev Mater Res 29(1):327–352
8. Corni I, Ryan MP, Boccaccini AR (2008) Electrophoretic deposition: from traditional ceramics to nanotechnology. J Eur Ceram Soc 28(7):1353–1367
9. Morefield SW, Hock VF, Weiss CA, Malone PG Application of electrokinetic nanoparticle migration in the production of novel concrete-based composites. In: AIP Conf Proc, 2008. pp 266–271
10. Ma J, Wang C, Peng K (2003) Electrophoretic deposition of porous hydroxyapatite scaffolds. Biomater 24:3505–3510
11. Chen C-Y, Chen S-Y, Liu D-M (1999) Electrophoretic deposition forming of porous alumina membranes. Acta Mater 47(9):2717–2726
12. Barthelat F, Tang H, Zavattieri PD, Li C-M, Espinosa HD (2007) On the mechanics of mother-of-pearl: a key feature in the material hierarchical structure. J Mech Phys Sol 55(2):306–337
13. Allison PG, Rodriguez RI, Hodo WD, Kennedy AJ, Chandler MQ, Hidalgo RG, Moser RD, Peters JF Structure and mechanical properties of biological multi-layered material systems. In: Khan AS (ed) 18th International Symposium on Plasticity and its Current Applications, San Juan, PR, 2012. I. J. Plast., pp 199–201
14. Moser RD, Weiss Jr CA, Chandler MQ, Hodo WD, Malone PG, Chappell MA, Seiter JM, Lafferty B, Rodriguez RI, Negron OR, Torres-Cancel KA, Hidalgo-Hernandez RG Application of advanced characterization tools to the study of structural biomaterials and bio-inspired materials. In: 4th Int Symp Nanotechnol Const, 2012
15. Watanabe J, Akashi M (2008) Controlled deposition of calcium carbonate particles on porous membranes by using alternative current system. J Coll Int Sci 327(1):44–50
16. ASTM (2006) C642: Standard test method for density, absorption, and voids in hardened concrete
17. Fyfe WF, Bischoff JL The calcite-aragonite problem. In: SEPM Spec Pub, 1965. pp 3–13
18. MacInnes DA (1939) The principles of electrochemistry. Dover, New York
19. Tai CY, Chen FB (1998) Polymorphism of CaCO3 precipitated in a constant-composition environment. AIChE J 44(8):1790–1798
20. Weiss Jr CA, Moser RD, Malone P, Torres-Cancel K, Allison PG, Chandler MQ, Hidalgo RG (2012) Production of mixed carbonate phases using ammonium carbonate-metal acetate reactions. Bioinsp, Biomimet and Nanobiomater Accepted
21. Sawada K (1997) The mechanisms of crystallization and transformation of calcium carbonates. Pure Appl Chem 69(5):921–928
22. Park RJ, Meldrum FC (2004) Shape-constraint as a route to calcite single crystals with complex morphologies. J Mater Chem 14(14):2291–2296
23. Yanagishita H, Negishi H, Yokokawa H (2002) Electrophoretic deposition of solid oxide fuel cell material powders. In: Proc Electrochemical Soc on Electrophoretic Depos: Fundamentals and Applications, Pennington, NJ, USA, pp 214–221